

STRESS ANALYSIS AND SIMULATION ON PIEZOELECTRIC QUARTZ WAFER UNDER MULTIDIMENSIONAL FORCES

Li Dong¹, Ren Zongjin¹, Jia Zhenyuan^{1*}, Zhao Liqi¹, Wang Fei¹

¹Key Laboratory for Precision & Nontraditional Machining of Ministry of Education,

Dalian University of Technology, Linggong Road 2nd, 116023, Dalian, China

*e-mail: dong.50121@hotmail.com

Abstract. Based on mechanics of anisotropic material and Maxwell's electromagnetic theory, the piezoelectric effect of piezoelectric material (SiO_2) under multidimensional forces has been studied. Exploring the distributions of stress field and polarization electric field inside the circular wafer, the piezoelectric equations between forces and induced charge on wafer's surface are established. Then the simulation analysis is performed by the FEM, obtaining polarization electric field and electric potential in the wafer. Results of both analyses show that if dividing the wafer's surface into four areas, the quantity of electric charge on each area is linearly related to bending moments and normal force, which gives a new way to measure multidimensional forces by a single quartz wafer. The study also provides the theoretical feasibility for developing a novel small-size multidimensional forces sensor.

1. Introduction

Currently, the researches on the piezoelectric effect are mainly based on the effects of stretching, compression and shearing, focused on the exploration of the input rule on the wafer under single force or moment, and sorts of piezoelectric sensors are developed, such as single-component sensor, three -component sensor, single-component torque sensor and their combinations. While the traditional multidimensional forces sensors usually consist of four three-component sensors or six single -component sensors, the large size of which limits their application in some narrow space, so it is urgent to develop smaller ones. It is discovered that the distribution of the induced charge on the surface of quartz wafer under multidimensional forces shows the regularity, and few published articles report the regularity. If the regularity can be studied and grasped, it will provide the theoretical support for development of the novel small-size multidimensional forces sensors.

Under multidimensional forces, 3-D composition effect will exist in quartz wafer, including tension and compression, bending, torsion and shearing. The researchers abroad led the studies on the bending effect and torsion effect on the piezoelectric quartz wafer. The former Soviet Union's researcher S.G. Lekhnitskii [1] conducted stress analysis to the anisotropic materials under the combined effect of bending moment and torque, building the mathematical model of the anisotropic body under 3-D forces; Jan Söderkvist [2-4] in Uppsala University, Sweden and Hirofumi Kawashima [5], Japan studied the bending vibration and torsional vibration of quartz wafer under the different drive electrode configurations, which were the most typical researches on bending and torsion effect. Reinhard Lerch [6] in Friedrich-Alexander University, Germany did the piezoelectric simulation research on the 2-D and 3-D finite elements models. The domestic researches on the piezoelectric effect are later, Dr. Sun Baoyuan [7-10] in Dalian University of Technology worked on the theories and

applications of piezoelectric effect, confirming the existence of bending effect and torsion effect in the quartz wafer and establishing the function of load-induced charge respectively. All these studies have promoted the development of the effect of bending and torsion, but basically they are still the single-moment researches, lack of further researches on the piezoelectric theory under 6-D forces.

This paper regards the X0-cut α -dextrorotation circular quartz wafer as the study object. Aimed at the anisotropic property of the quartz wafer, the piezoelectric effect of single-piece wafer under 6-D forces is explored, then simulation research is performed by Ansys, acquiring a result matched with the former. The result of theoretical analysis and simulation will provide the theoretical basic for realizing the measurement of multidimensional forces by single piece of quartz wafer or a pair, enriching the field of piezoelectric sensors greatly.

2. Stress mathematical model of the quartz wafer under 6-D forces

For the isotropic material, bending moment is independent to torque within small deformation, and the total deformation and the stress can be obtained by the superposition of both effects; While for the anisotropic material, bending moment will couple with torque within small deformation, that is to say torque will generate bending deformation and bending moment will lead to torsion deformation.

Quartz belongs to the anisotropic material, when only three moments are applied on it, the coupling of the moments needs to be analyzed, the wafer model is shown in Fig. 1.

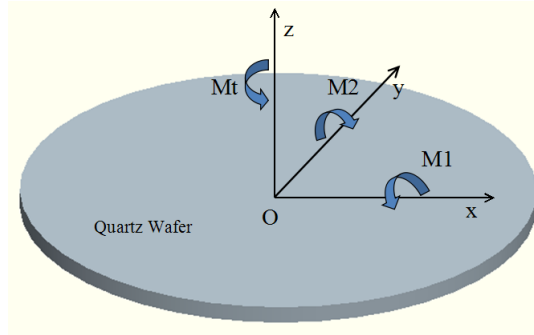


Fig. 1. Model of quartz wafer under 3-D forces.

According to the mechanics of anisotropic material, this is a spacial bending-torsion case, including the generalized plane strain problem and generalized torsion problem [1]. According to the differential equations and the boundary conditions of both problems, each component in the stress field can be got from equation (1).

$$\left\{ \begin{array}{l} \sigma_x = \frac{\partial^2 F}{\partial y^2} + \bar{U}, \quad \sigma_y = \frac{\partial^2 F}{\partial x^2} + \bar{U}, \quad \tau_{xy} = -\frac{\partial^2 F}{\partial x \partial y} \\ \tau_{xz} = \frac{\partial \psi}{\partial y}, \quad \tau_{yz} = -\frac{\partial \psi}{\partial x} \\ \sigma_z = \left(\frac{s_{34}}{2s_{33}} M_t - M_2 \right) \frac{x}{I_2} + \left(-\frac{s_{35}}{2s_{33}} M_t + M_1 \right) \frac{y}{I_1} - \\ \frac{1}{s_{33}} (s_{13}\sigma_x + s_{23}\sigma_y + s_{34}\tau_{yz} + s_{35}\tau_{xz} + s_{36}\tau_{xy}) \end{array} \right., \quad (1)$$

wherein, F represents the plane stress function, while ψ represents torsion function, I_1 ,

I_2 are the principal moments of inertia of wafer for the x and y axis respectively, M_1 , M_2 are the torques for x and y axis respectively, M_t is the torque for z axis, s_{ij} is elastic compliance coefficient, \bar{U} is volume and face force.

After determining the stress distribution within the wafer under the three moments, the stress field of wafer under 6-D forces is analyzed. The 6-D forces applied on the wafer consist of three directional forces (the normal force F_z and the tangential force F_x and F_y) and three moments (the torque M_t and the bending moment M_1 and M_2), the mechanical model is shown in Fig. 2.

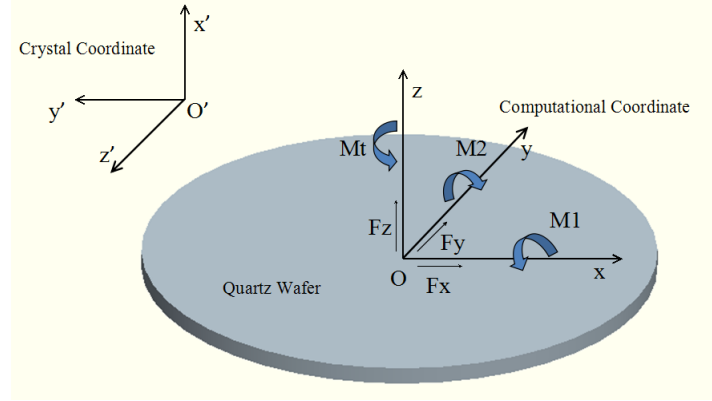


Fig. 2. Model of the quartz wafer under 6-D forces.

As on the side face of the wafer no pulling or compressing stress in x and y directions are applied on the wafer and no volume or face forces exist on the lateral surface, so $F=0$ and $\bar{U}=0$. According to the independence and the superposition of stresses and based on equation(1), the final stress mathematical model of quartz wafer under 6-D forces is acquired as equation(2).

$$\left\{ \begin{array}{l} \sigma_x = 0 \\ \sigma_y = 0 \\ \sigma_z = \left(\frac{s_{34}}{2s_{33}} M_t - M_2 \right) \frac{x}{I_2} + \left(-\frac{s_{35}}{2s_{33}} M_t + M_1 \right) \frac{y}{I_1} - \\ \frac{1}{s_{33}} (s_{13}\sigma_x + s_{23}\sigma_y + s_{34}\tau_{yz} + s_{35}\tau_{xz} + s_{36}\tau_{xy}) + \frac{F_z}{A} \\ \tau_{yz} = -\frac{\partial \psi}{\partial x} + \frac{F_y}{A} \\ \tau_{xz} = \frac{\partial \psi}{\partial y} + \frac{F_x}{A} \\ \tau_{xy} = 0 \end{array} \right. \quad (2)$$

wherein, A represents the area of the upper face of the wafer, F_x and F_y are the tangential forces on the plane xy, pointing to the x and y positive direction respectively, F_z represents the normal force on the plane xy, pointing to the z positive direction.

3. Numerical calculation and simulation analysis by Matlab

Numerical calculation of piezoelectric effect. The paper studies the X0-cut α -dextrorotation circular quartz wafer, with the radius $r=15$ mm and the thickness $h=1$ mm. The theoretical stress calculation in last chapter is done in the computational coordinate O_{xyz} , as shown in Fig. 2. While the characteristic constants of the wafer are defined in the crystal coordinate $O'x'y'z'$. For the convenience of calculation, the crystal coordinate needs to be transformed into the computational coordinate, obtaining the characteristic constants in new coordinate. In the computational coordinate O_{xyz} , the elastic compliance coefficient matrix s and the piezoelectric coefficient matrix d are listed as follow respectively:

$$s = \begin{bmatrix} 12.77 & -1.22 & -1.79 & 0 & 0 & 4.5 \\ -1.22 & 9.6 & -1.22 & 0 & 0 & 0 \\ -1.79 & -1.22 & 12.77 & 0 & 0 & -4.5 \\ 0 & 0 & 0 & 20.04 & -9.0 & 0 \\ 0 & 0 & 0 & -9.0 & 29.12 & 0 \\ 4.5 & 0 & -4.5 & 0 & 0 & 20.04 \end{bmatrix} \times 10^{-12} m^2 / N$$

$$d = \begin{bmatrix} 0 & 0 & 0 & -0.727 & 4.62 & 0 \\ 0 & 0 & 0 & 0 & 0 & 0 \\ 2.31 & 0 & -2.31 & 0 & 0 & 0.727 \end{bmatrix} \times 10^{-12} C / N$$

For the X0-cut quartz wafer, the normal stress on plane z σ_z is listed as equation (3):

$$\sigma_z = \left(\frac{s_{34}}{2s_{33}} M_t - M_2 \right) \frac{x}{I_2} + \left(-\frac{s_{35}}{2s_{33}} M_t + M_1 \right) \frac{y}{I_1} - \frac{1}{s_{33}} (s_{13}\sigma_x + s_{23}\sigma_y + s_{34}\tau_{yz} + s_{35}\tau_{xz} + s_{36}\tau_{xy}) + \frac{F_z}{A} \quad (3)$$

Although, torque M_t will produce two tangential stresses τ_{zy} and τ_{zx} on the plane z , while in current computational coordinate, the elastic compliance coefficient $s_{33} \neq 0$, $s_{34} = s_{35} = 0$, by simplifying equation(3), equation(4) is acquired as follow:

$$\sigma_z = -\frac{M_2 x}{I_2} + \frac{M_1 y}{I_1} + \frac{F_z}{A}. \quad (4)$$

From equation(4), it is obvious that torque M_t and tangential forces F_x and F_y make no effect on the normal stress σ_z , and no coupling exists between bending moments and torque. So in the computational coordinate, the simplified stress situation of X0-cut wafer under 6-D forces is listed as equation(5):

$$\left\{ \begin{array}{l} \sigma_x = 0 \\ \sigma_y = 0 \\ \sigma_z = -\frac{M_2^x}{I_2} + \frac{M_1^y}{I_1} + \frac{F_z}{A} \\ \tau_{yz} = -\frac{\partial \psi}{\partial x} + \frac{F_y}{A} \\ \tau_{xz} = \frac{\partial \psi}{\partial y} + \frac{F_x}{A} \\ \tau_{xy} = 0 \end{array} \right. , \quad (5)$$

wherein, the axial moment of inertia $I_1=I_2=\pi r^4/4$.

The intensity of polarization P can be calculated by equation (6) listed as follow:

$$P = dT, \quad (6)$$

wherein, d represents the piezoelectric coefficient matrix in coordinate $Oxyz$, T is the load matrix, $T = [\sigma_x \ \sigma_y \ \sigma_z \ \tau_{yz} \ \tau_{xz} \ \tau_{xy}]^T$.

The density of induced charge on the plane z of the wafer η_p can be calculated by equation (7) listed as follow:

$$\eta_p = P \cdot e, \quad (7)$$

wherein, e is the unit normal vector.

The z -component of the intensity of polarization P_z can be acquired by equation (5) and equation(6):

$$P_z = d_{31}\sigma_x + d_{33}\sigma_z + d_{36}\tau_{xy} = d_{33}\left(-\frac{M_2^x}{I_2} + \frac{M_1^y}{I_1} + \frac{F_z}{A}\right). \quad (8)$$

According to the equation(7) and (8), η_{z+} , η_{z-} can be calculated, listed as equation(9), referring to the density of induced charge on the upper face “ $z+$ ” and the bottom face “ $z-$ ” of the wafer in the z -direction respectively.

$$\left\{ \begin{array}{l} \eta_{z+} = P \cdot n = P_z \cdot e_z = d_{33}\left(-\frac{M_2^x}{I_2} + \frac{M_1^y}{I_1} + \frac{F_z}{A}\right) \\ \eta_{z-} = P \cdot n = -P_z \cdot e_z = -d_{33}\left(-\frac{M_2^x}{I_2} + \frac{M_1^y}{I_1} + \frac{F_z}{A}\right) \end{array} \right. , \quad (9)$$

wherein, $d_{33} = -2.31 \times 10^{-12} \text{ C/N}$, $I_1 = I_2 = \pi r^4 / 4 = 4.0 \times 10^{-8} \text{ m}^4$.

Divide the upper face “ $z+$ ” into four areas, which are area1, area2, area3 and area4 respectively, as shown in Fig. 3.

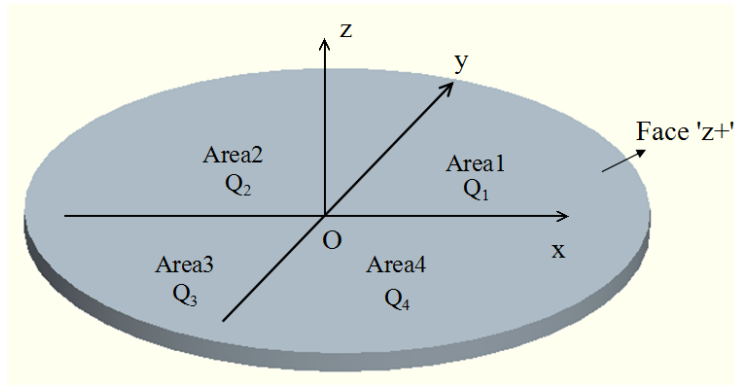


Fig. 3. Four divided areas on upper face “z+”.

Q_1 , Q_2 , Q_3 and Q_4 are the quantity of electric charge in the four areas respectively, which can be calculated by integrating the density of induced charge η_{z+} obtained by equation(9) in the four areas respectively. The results are listed as equation(10):

$$\begin{aligned}
 Q_1 &= \iint_{z+_{xy}} \eta_{z+} dxdy = [0.654(M_2 - M_1) - 0.0058F_z] \times 10^{-10} (C) \\
 Q_2 &= \iint_{z+_{-x,y}} \eta_{z+} dxdy = [-0.654(M_1 + M_2) - 0.0058F_z] \times 10^{-10} (C) \\
 Q_3 &= \iint_{z+_{-x,-y}} \eta_{z+} dxdy = [0.654(M_1 - M_2) - 0.0058F_z] \times 10^{-10} (C) \\
 Q_4 &= \iint_{z+_{x,-y}} \eta_{z+} dxdy = [0.654(M_2 + M_1) - 0.0058F_z] \times 10^{-10} (C)
 \end{aligned} \tag{10}$$

Observing the theoretical results above, it is clear that for X0-cut quartz wafer under 6-D forces, the quantity of electric charge induced on the surface of the wafer is strictly linearly related to bending moments M_1 , M_2 and the normal force F_z . Assigning $M_1=M_2=10N.m$, $F_z=-1000N$ in equation (10), the results can be obtained as follow:

$$Q_1 = 5.8 \times 10^{-10} C, Q_2 = -7.28 \times 10^{-10} C, Q_3 = 5.8 \times 10^{-10} C, Q_4 = 18.88 \times 10^{-10} C.$$

When two bending moments and normal force applied on the quartz wafer, by laying out four electrode slices on the four areas of the top “z+” and detecting Q_1 , Q_2 , Q_3 , Q_4 , it is easy to get M_1 , M_2 and F_z , listed as equation (11).

$$\begin{aligned}
 M_1 &= 3.84(-Q_1 - Q_2 + Q_3 + Q_4) \times 10^9 (N \cdot m) \\
 M_2 &= 3.84(Q_1 - Q_2 - Q_3 + Q_4) \times 10^9 (N \cdot m) \\
 F_z &= -4.31(Q_1 + Q_2 + Q_3 + Q_4) \times 10^{11} (N)
 \end{aligned} \tag{11}$$

Simulation analysis by Matlab. By applying the Matlab PDE toolbox, the paper has conducted the numerical analysis of the polarization electric field and the electric potential qualitatively, depicting visually the distribution of the electric field and potential on the surface of the quartz wafer under multidimensional forces.

According to the rule followed by the electrostatic field when there exists material [11], the electric field produced by the equivalent bound charge under 6-D forces meets the Maxwell's equations. Within the quartz wafer, the electric potential meets the anisotropic differential control equation (Poisson's equation), shown as equation (12).

$$\sum_{i=1}^3 \sum_{j=1}^3 \varepsilon_{ij} \frac{\partial^2 V(r)}{\partial x_i \partial x_j} = -\frac{\rho_p}{\varepsilon_0}, \quad (12)$$

wherein, ρ_p is the polarized body density of induced charge, ε_{ij} represents the dielectric coefficient with $\varepsilon_{11}=\varepsilon_{22}=4.52$, $\varepsilon_{33}=4.62$ for quartz wafer, $V(r)$ is electrostatic field scalar potential in the anisotropic medium, ε_0 is dielectric constant.

The polarized body density of charge ρ_p can be obtained by equation (13):

$$\rho_p = -\nabla \cdot \mathbf{P} = -\left(\frac{\partial P_x}{\partial x} + \frac{\partial P_y}{\partial y} + \frac{\partial P_z}{\partial z}\right). \quad (13)$$

From the theoretical result of the induced charge calculated in the previous chapter it is known that for X0-cut quartz wafer under 6-D forces, the quantity of the induced charge on the wafer surface is only related to the bending moments M_1 , M_2 and the normal force F_z , so in the numerical analysis of electric potential, it's enough to apply only the three forces on the quartz wafer. By equation (4), the normal stress σ_z can be obtained, and the values of other five stresses are all zero. Finally by equation (6), (7) and (13), it can be calculated that $\rho_p = 0$.

When $\rho_p = 0$, the differential equation(12) can be transformed into Laplace's equation, listed as equation (14):

$$\sum_{i=1}^3 \sum_{j=1}^3 \varepsilon_{ij} \frac{\partial^2 V(r)}{\partial x_i \partial x_j} = 0. \quad (14)$$

The boundary condition in the electrostatic is listed as equation (15):

$$\left. \begin{aligned} n \cdot (\varepsilon_0 \varepsilon_r E_1 - \varepsilon_0 \varepsilon_r E_2) &= \eta_p \\ n \cdot (E_1 - E_2) &= 0 \end{aligned} \right\}, \quad (15)$$

wherein, η_p is the facial density of induced charge, $\varepsilon_r = \varepsilon_{ij} e_i e_j$, E is the electric field.

By applying the Matlab PDE toolbox and assigning $M_1 = M_2 = 10 \text{ N} \cdot \text{m}$, $F_z = -1000 \text{ N}$, the equation (14) can be solved under the boundary condition equation (15), acquiring the results shown in Fig. 4.

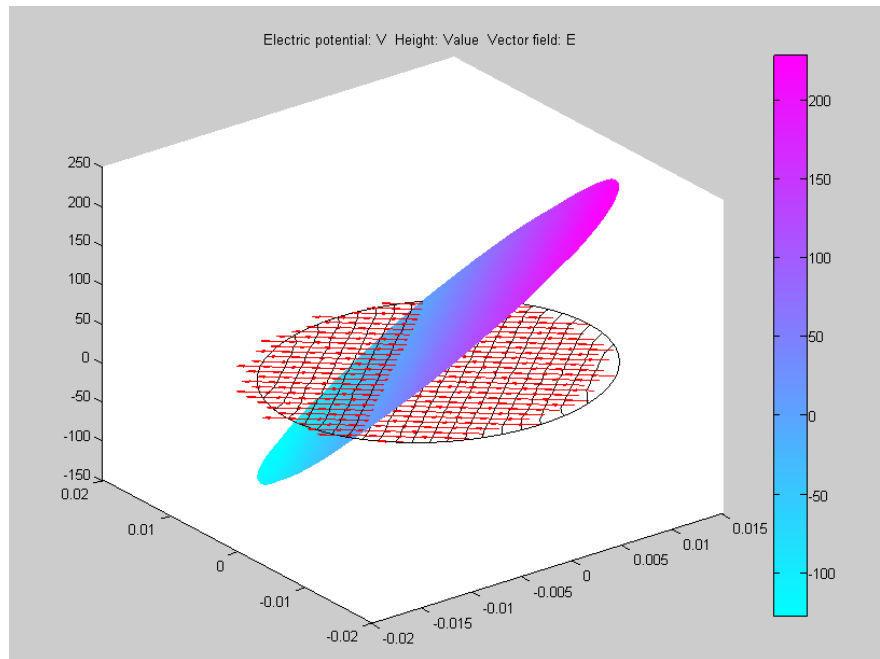


Fig. 4. Equipotential diagram of electric potential and electric field on face “z+”.

From Fig. 4, it is obvious that the electric potential shows that the fourth quadrant has the highest electric potential with the lowest in the second quadrant, and the deeper the color of the area turns, the higher electric potential the area has, presenting a symmetrical distribution along the line $x + y = 0$ (in the numerical coordinate), which is in accord with the distribution of quantity of electric charge calculated by equation (10). Figure 4 also shows the distribution of electric field vector with the direction from high potential to low potential.

4. Simulation research on the quartz wafer by the FEM

In the simulation research by the software of FEM, Ansys, the X0-cut α -dextrorotation circular quartz wafer is analyzed, with the radius $r = 15$ mm and the thickness $h = 1$ mm. The model of the quartz wafer is established in the numerical coordinate O_{xyz} . According to the rule of coordinate transformation, the stiffness matrix and piezoelectric coefficient matrix can be obtained in current coordinate.

When defining the material properties, the element type Solid5 should be chosen, which is special for piezoelectric simulation. When modeling, the whole circular wafer consists of four 1/4 wafers, convenient for mapped meshing, as Fig. 5a shows.

For the purpose of checking and comparing the results of electric potential on the four areas more clearly, couple the electric potential of all nodes on each area respectively and build a node on each of the four areas, which are node1 ($0.6r, 0.6r, h$), node2 ($-0.6r, 0.6r, h$), node3 ($-0.6r, -0.6r, h$) and node4 ($0.6r, -0.6r, h$) respectively, as shown in Fig. 5b.

After the model is built, the loading step and solving step are followed. First, the displacement of the wafer should be restricted. So the degrees of freedom (U_x, U_y, U_z, VOL) of all the nodes on the bottom “z-” of the wafer are set to zero. As the induced charge on the surface of the wafer is only related to the bending moments M_1, M_2 and the normal force F_z , so in the simulation analysis, just the three forces need to be applied on the wafer.

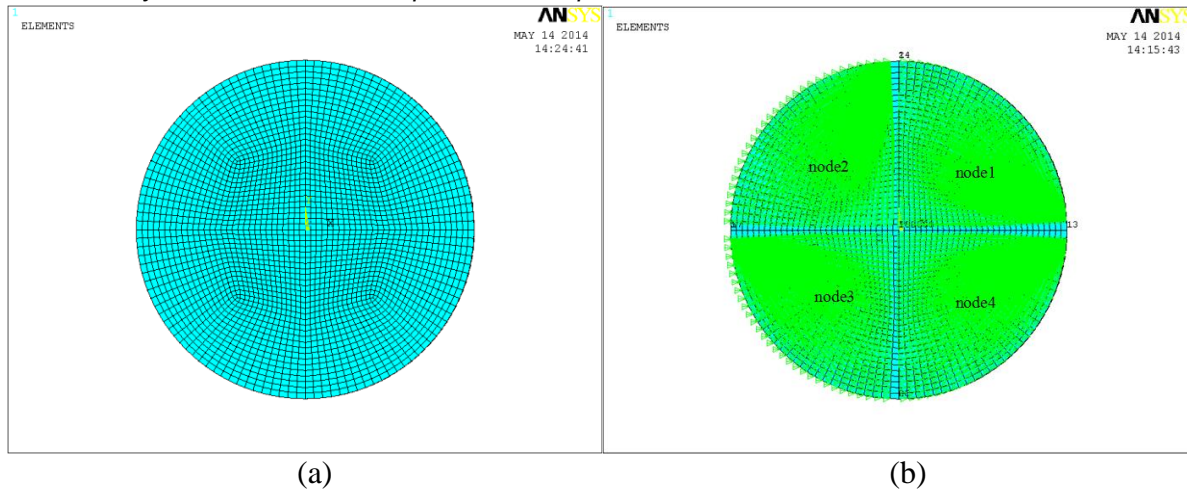
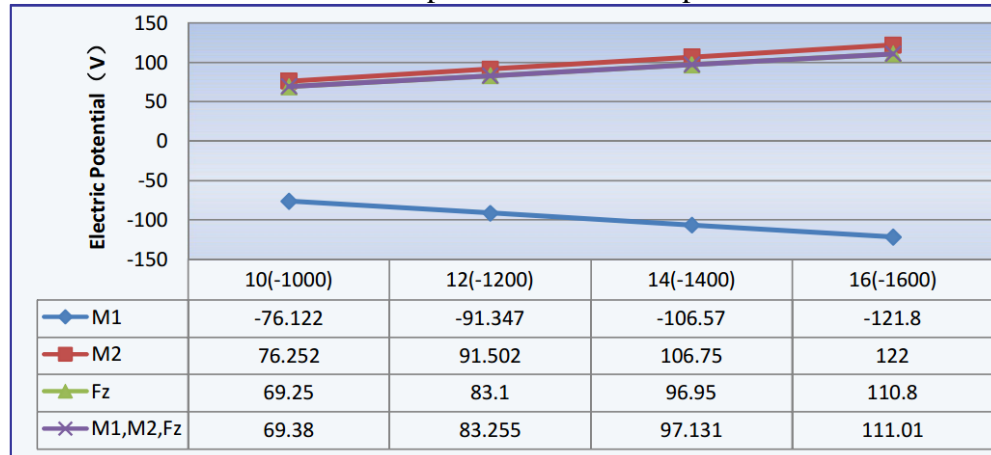


Fig. 5. (a) The finite element model of wafer;
(b) The coupling model of the wafer with four nodes.

The specific process of loading is: Firstly, apply M_1 , M_2 and F_z on the quartz wafer separately. The numerical values of both moments are 10, 12, 14, 16 $N \cdot m$ in sequence and that of the normal force F_z is -1000, -1200, -1400, -1600 N in sequence. Then apply M_1 , M_2 and F_z on the quartz wafer simultaneously with initial numerical value 10 $N \cdot m$, 10 $N \cdot m$, -1200 N respectively, increasing at the same extent as applied separately. After all the loads are applied, solve and check the results of the nodes, four sets of load-potential data can be obtained at each of the four built nodes. The relationships between load and electric potential at node 1-4 are shown as chart 1-4 respectively.

Chart 1. The load-potential relationship on node1.



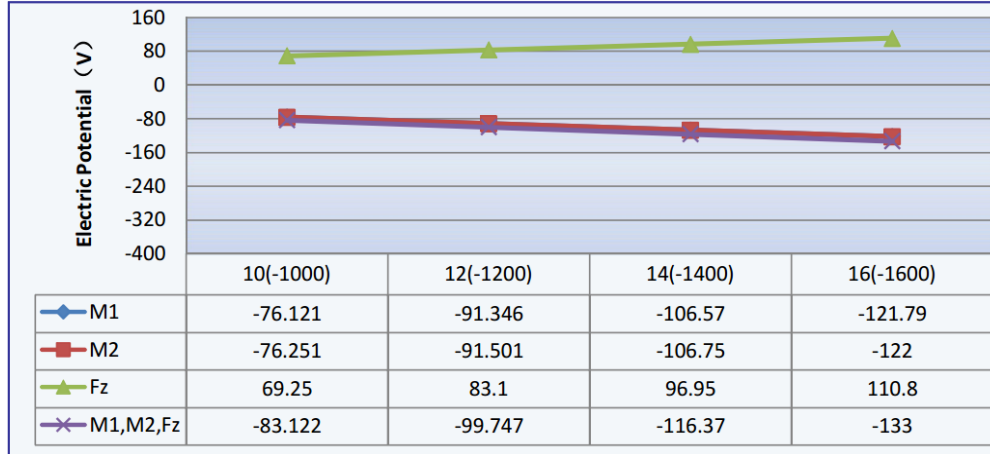
*Line " F_z " basically coincides with Line " M_1, M_2, F_z ".

It is obvious from chart 1-4 that for each node, the superposition of each effect made by single load applied on the wafer equals to the combined effect made by all loads applied simultaneously on the wafer.

When all loads are applied on the wafer, the electric potential on node1 is positive, corresponding to the positive charge quantity Q_1 on area1 calculated by equation(10); The electric potential on node2 is negative, corresponding to the negative charge quantity Q_2 on

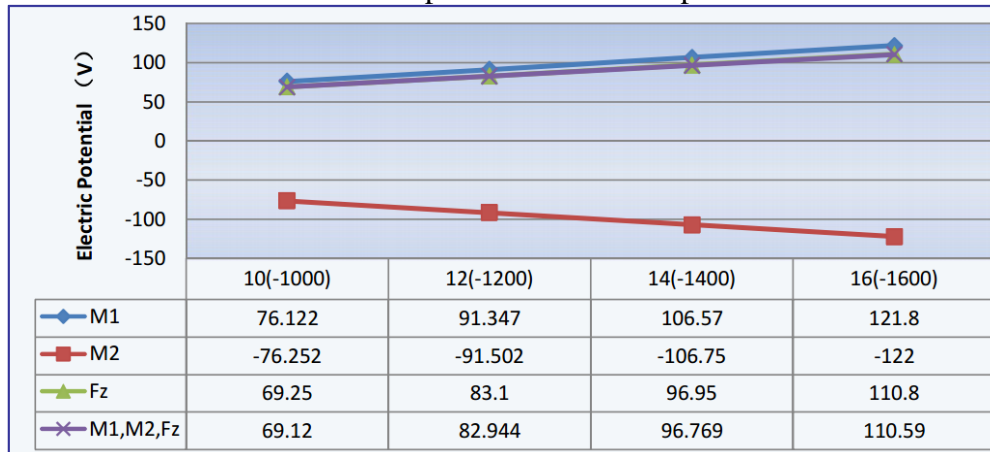
area2; The electric potential on node3 is positive, corresponding to the positive charge quantity Q_3 on area3; The electric potential on node4 is positive, corresponding to the positive charge quantity Q_4 on area 4.

Chart 2. The load-potential relationship on node2.



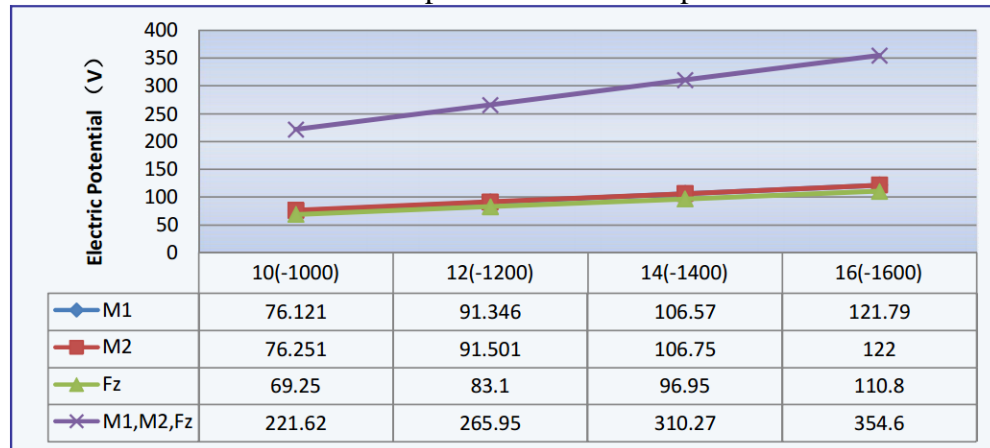
* Line " M_1 " basically coincides with Line " M_2 ".

Chart 3. The load-potential relationship on node3.



* Line " F_z " basically coincides with Line " M_1, M_2, F_z ".

Chart 4. The load-potential relationship on node4.



*Line " M_1 " basically coincides with Line " M_2 ".

Figures 6 and 7 separately show the electric potential contour and electric field vector

contour of the quartz wafer under both the moments ($M_1 = M_2 = 16N \cdot m$) and the normal force ($F_z = -1600N$) simultaneously. From Fig. 6 and Fig. 7, it is obvious that area2 has the highest electric potential with the vector of electric field pointing down and the area4 has the lowest potential with the vector of electric field pointing up. All the results of simulation by Ansys match well with the theoretical analysis.

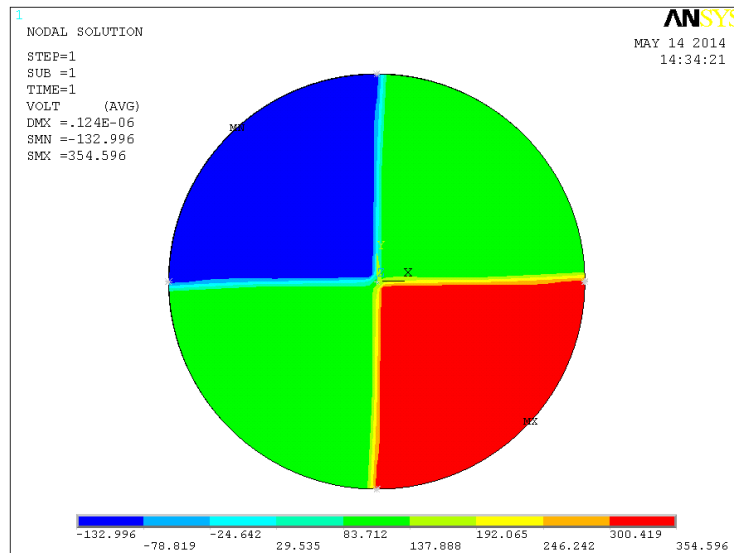


Fig. 6. Electric potential contour
($M_1 = M_2 = 16N \cdot m$, $F_z = -1600N$).

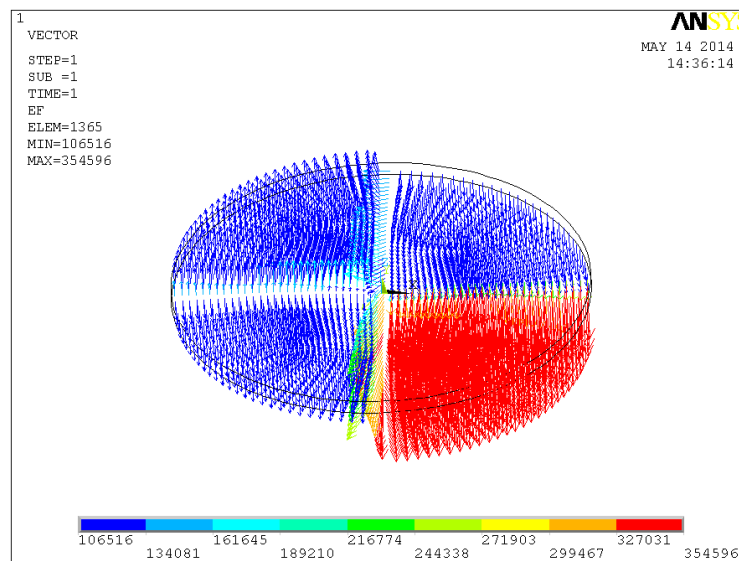


Fig. 7. Electric field vector contour
($M_1 = M_2 = 16N \cdot m$, $F_z = -1600N$).

5. Conclusions

By analyzing the stress state of the quartz wafer under multidimensional forces, the mathematical equations are established between the multidimensional forces and the induced charge on the surface of the wafer, acquiring the theoretical results, and then the simulation research is conducted with Ansys. The results show that for X0-cut quartz wafer under 6-D forces, the bending moments and the normal force can generate the induced charge on the

surface of the wafer, while the torque and the tangential forces cannot. Attaching four electrode slices to the four areas on the surface of X0-cut wafer separately with the wires connected, a simple multidimensional forces-measured sensor is made, which can realize the measurement of the bending moments M_1 , M_2 and the normal force F_z by measuring the quantity of electric charge on each of the four areas. Based on the simple model and through the designation and optimization, a novel and small-size multidimensional sensor will be invented, which can be widely used in kinds of small space in the engineering field.

Acknowledgements

The authors gratefully acknowledge the financial supports of the National Natural Science Found of China (No.51205044) and Specialized Research Fund for the Doctoral Program of Higher Education (20120041120058).

References

- [1] S.G. Lekhniskii, *Theory of elasticity of an anisotropic body* (Mir publishers, Moscow, 1981).
- [2] Jan Söderkvist // *Measurement Science and Technology* **1** (1990) 731.
- [3] Jan Söderkvist // *IEEE Transactions on Ultrasonics Ferroelectrics-Frequency control* **38(3)** (1991) 271.
- [4] Jan Söderkvist // *Sensors and Actuators A* **32** (1992) 567.
- [5] Hirofumi Kawashima, Kenji Sunaga // *IEEE Transactions on Ultrasonics, Ferroelectrics, and Frequency Control* **43(5)** (1996) 832.
- [6] Reinhard Lerch // *IEEE Transactions on Ultrasonics, Ferroelectrics and Frequency Control* **37(2)** (1990) 233.
- [7] Gao Changyin, Liwanquan, Sun Baoyuan // *Measurement* **43** (2010) 336.
- [8] Wu Jiantong, Sun Baoyuan // *Journal of Dalian University of Technology* **41(2)** (2001) 187.
- [9] Gao Changyin, Sun Baoyuan // *Chinese Journal of Mechanical Engineering* **40(8)** (2004) 151.
- [10] Wang Yingguang, Sun Baoyuan // *Piezoelectrics and Acoustooptics* **25(4)** (2003) 308.
- [11] William H. Hayt, John A. Buck, *Engineering electromagnetic* (McGraw Hill Higher Education, Boston, 2006).